PHYSICAL REVIEW B **91**, 220403(R) (2015)

Direct observation of noncollinear order of Co and Mn moments in multiferroic $Mn_{0.85}Co_{0.15}WO_4$

J. Herrero-Martín,[1,2] A. N. Dobrynin,[3] C. Mazzoli,[4] P. Steadman,[3] P. Bencok,[3] R. Fan,[3] A. A. Mukhin,[5] V. Skumryev,[6,7] and J. L. García-Muñoz[2]

[1]*ALBA Synchrotron Light Source, Ctra. BP 1413, km 3.3, E-08290 Cerdanyola del Vallès, Barcelona, Spain*

[2]*Institut de Ciència de Materials de Barcelona (ICMAB-CSIC), E-08193 Bellaterra, Barcelona, Spain*

[3]*Diamond Light Source Ltd., Harwell Science and Innovation Campus, Didcot OX11 0DE, United Kingdom*

[4]*Dipartimento di Fisica, Politecnico di Milano, Piazza Leonardo da Vinci, 32, I-20133 Milano, Italy*

[5]*Prokhorov General Physics Institute, Russian Academy of Science, Vavilov Street, 38, 119991 Moscow, Russian Federation*

[6]*Institució Catalana de Recerca i Estudis Avançats, E-08010 Barcelona, Spain*

[7]*Departament de Física, Universitat Autònoma de Barcelona, E-08193 Bellaterra, Barcelona, Spain*

(Received 3 February 2015; revised manuscript received 1 May 2015; published 3 June 2015)

Doping $Mn_{1-x}Co_xWO_4$ with Co produces a rich magnetic phase diagram with a large number of ferroelectric phases. We present resonant x-ray magnetic scattering experiments in the known collinear AF4 phase of multiferroic $Mn_{0.85}Co_{0.15}WO_4$ showing that Mn and Co spins point to different directions despite they randomly occupy the same crystallographic site. The resultant noncollinear exotic spin configuration is determined by a competition of Mn^{2+} and Co^{2+} magnetic anisotropies and demands a reexamination of the ferroelectric phase diagram of this model family beyond the previous average description of its magnetic orders.

DOI: 10.1103/PhysRevB.91.220403 PACS number(s): 75.85.+t, 75.25.−j, 75.50.Ee

Materials with magnetic frustration and complex magnetic orders breaking the spatial inversion symmetry attract great interest as an effective source of multiferroic (MF) and magnetoelectric (ME) properties [1–4]. Magnetically frustrated $MnWO_4$ (Hübnerite) and the (Mn, Co)WO_4 extended family are reference models to study the interaction between spins and polar orders and to investigate the magnetic control of electric polarization [5–9]. They present monoclinic crystal structure ($P2/c$), where Mn and Co cations occupy the same $2f$ site and are surrounded by distorted oxygen octahedra aligned in zigzag chains along the c axis [10,11]. Noncollinear magnetic order in these compounds is a consequence of magnetic frustration due to their geometry and the contest between distinct exchange intrachain and interchain coupling terms of Heisenberg type and uniaxial anisotropy [12]. Thanks to their simple structure and rich ferroelectric (FE) behavior emergent ideas and phenomena involved in the ME response of improper MFs can be revealed or tested [5–16]. Among all $Mn_{1-x}M_xWO_4$ (M: transition-metal) isostructural compounds with magnetic and nonmagnetic substitutions, Co generates the most complex and rich phase diagrams [5–18], and its large magnetocrystalline anisotropy has been hold responsible for it. $CoWO_4$ is a collinear antiferromagnet isostructural to the manganese-based parent FE system [17]. Soft x-ray absorption experiments and multiplet calculations established that the Co^{2+} single-ion anisotropy here favors collinear order due to the spin-orbit coupling effect over the orbital moment [18]. So, in $Mn_{1-x}Co_xWO_4$, isotropic Mn^{2+}-Mn^{2+} exchange interactions compete with the uniaxial Co magnetic anisotropy giving rise to various competing MF phases with complex magnetic orders: antiferromagnetic (AF), modulated, cycloidal, and conical. $MnWO_4$ undergoes three successive magnetic transitions on decreasing temperature into AF3, AF2 and AF1 phases, the first two with incommensurate propagation vectors to the crystal lattice. The paraelectric AF1 phase is commensurate [$\mathbf{k} = (\pm 1/4, 1/2, 1/2)$] and presents collinear moments. It takes over the FE AF2 phase at low temperatures in $MnWO_4$, although AF1 gets rapidly suppressed by Co substitution ($x \geqslant 0.03$) [15,19]. The elliptical helix in AF2 (with the spins rotating in a plane perpendicular to the ac plane) is responsible for the FE phase dominating the T-x phase diagram in the first compositional block ($0 \leqslant x < 0.08$) at low temperatures. For $0.08 \leqslant x < 0.15$ the magnetocrystalline anisotropy increase induces a new orientation of the spins rotation plane (AF2', the spins now rotate parallel to the ac plane), which brings about a flop of the electrical polarization from the b axis (AF2) to the ac plane (AF2') [7,13,15]. Increasing temperature, both AF2 and AF2' briefly adopt a modulated collinear order (AF3, $T_C = 12\,\mathrm{K} < T < T_N = 13\,\mathrm{K}$) prior to becoming paramagnetic (PM). For x < 0.15 the longest (easy) axis of the elliptical helix remains in the ac plane, rotating from 56° ($x = 0$) to $\theta = 134°$ (as in $CoWO_4$) with increasing Co content. Last, for $x \geqslant 0.15$ AF2' disappears and $Mn_{1-x}Co_xWO_4$ samples are then dominated by the collinear order inherent to $CoWO_4$, AF4 [14,15,20]. Interestingly, in this region the collinear AF4 order [$\mathbf{k} = (1/2, 0, 0)$] first appears at T_N. Decreasing temperature, there is a ferroelectric transition at $T_C < T_N$ due to the appearance of the incommensurate AF2 cycloidal order (with spins rotating perpendicularly to the ac plane), which coexists with the collinear AF4 order below T_C. The juxtaposition for $x > 0.15$ of the collinear AF4 and incommensurate AF2 orders generates an AF conical structure [14] (with the collinear and cycloidal spin components being perpendicular). So, we will focus on $Mn_{0.85}Co_{0.15}WO_4$, of particular interest because it is regarded as the composition presenting maximum frustration in the family [15,20]. Besides the several competing magnetic orders in $Mn_{0.85}Co_{0.15}WO_4$, we must recall that the AF4 magnetic phase appears at $T_N \approx 17\,\mathrm{K}$, and coexists with the ferroelectric AF2 phase below $T_C = 10\,\mathrm{K}$ [20].

The (Mn, M)WO_4 families also constitute a reference example of intrinsically inhomogeneous MFs, where two different magnetic ions share the same crystallographic position. In this work we investigate the precise magnetic structure of a crystal with $Mn_{0.85}Co_{0.15}WO_4$ critical composition above its FE transition, exploiting chemical selectivity to move beyond

the average description provided by neutron diffraction. We present resonant x-ray magnetic scattering (RXMS) results at energies corresponding to $2p$ to $3d$ electronic transitions in Mn and Co ions in the so-called collinear AF4 phase. Its simplicity allowed us to study the individual orientation of both types of magnetic moments in great detail, demonstrating that Mn and Co spins point to different directions despite they randomly occupy the site.

The $Mn_{0.85}Co_{0.15}WO_4$ single crystal used was grown by the floating zone method, and cut with cuboid shape and surface normal vector [1 0 0]. RXMS was performed at the RASOR end station in I10 beam line of the diamond light source [21]. The crystal was mounted on the diffractometer with the [0 0 1] crystal axis along the beam propagation direction (for $\theta_{diff} = 0°$). Full polarization analysis was achieved by control of the incident light polarization provided by the undulator source and, following the scattering by the sample, further scattering at 90º by either of the two W/B4C multilayer polarization analyzers with periods optimized for working in Mn and Co $L_{2,3}$ absorption edges energies [21,22]. The scattered light was recorded by a photodiode. A liquid helium flow cryostat allowed sample cooling down to 12 K in ultrahigh vacuum conditions. Measurements were focused on the AF4 phase, above the FE transition ($T_C = 10$ K) induced by appearance of the AF2 cycloidal order.

We looked for spectral signatures of the magnetic reflection with wave vector (1/2 0 0) characteristic of the AF4 phase (magnetic cell doubled along the a axis) profiting from the resonant enhancement of weak magnetic x-ray diffraction signals at absorption edges. By working at core-to-valence $L_{2,3}$ edges of $3d$ transition metals we effectively probed magnetism at the electronic bands closest to the Fermi level. AF4 is the only magnetic phase accessible in $Mn_{0.85}Co_{0.15}WO_4$ where both Mn and Co $L_{2,3}$ absorption edges can be studied due to the reduced dimension of the propagation vector in the reciprocal space. The (1/2 0 0) magnetic reflection is observable beyond 645 eV, following Bragg's law. This range covers the Mn L_2, and the Co $L_{2,3}$ edges. The geometrical limitations arising from the multilayers setup for polarization analysis resulted in a small further reduction of this range in practice; however this did not compromise our experiment.

The top part of Fig. 1 shows the energy dependence of the (1/2 0 0) magnetic reflection intensity across the Mn L_2 edge at 13 K. The large resonant enhancement is a consequence of the Mn moments' long-range order. The spectrum is abnormally cut at 653 eV due to above commented limitations. In the bottom part of the same figure we see the corresponding spectrum across the Co $L_{2,3}$ edges. A large resonance peaks at 782 eV, directly demonstrating the existence of Co magnetic moments' long-range order with the same propagation vector as for Mn ones. The resonant spectral shape is typical of a Co^{2+}-based system, with a noticeable absence of any resonant enhancement at the Co L_2 edge. This is due to the electronic filling of Co $3d$ orbitals and it is actually a reliable indicator of the high spin state of Co^{2+} ions, with a large orbital momentum [23,24]. The same Co ions electronic configuration has been found in $CoWO_4$ [18].

A further proof of the magnetic origin of the spectral features in Fig. 1 can be found in their temperature evolution, displayed in Fig. 2. The resonances at both Mn L_2 and Co L_3

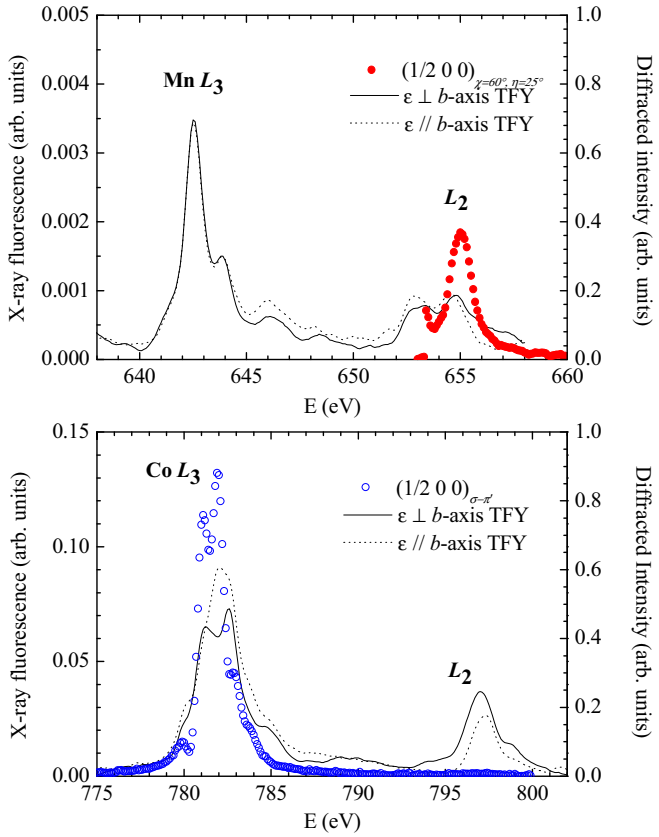

FIG. 1. (Color online) Energy dependence of (1/2 0 0) magnetic reflection intensity (symbols) at 13 K across Mn $L_{2,3}$ (top) and Co $L_{2,3}$ (bottom) edges. X-ray absorption spectra measured in total fluorescence yield (TFY) mode measured for σ (dotted lines) and π (solid lines) incident light polarization in each case are shown for comparison.

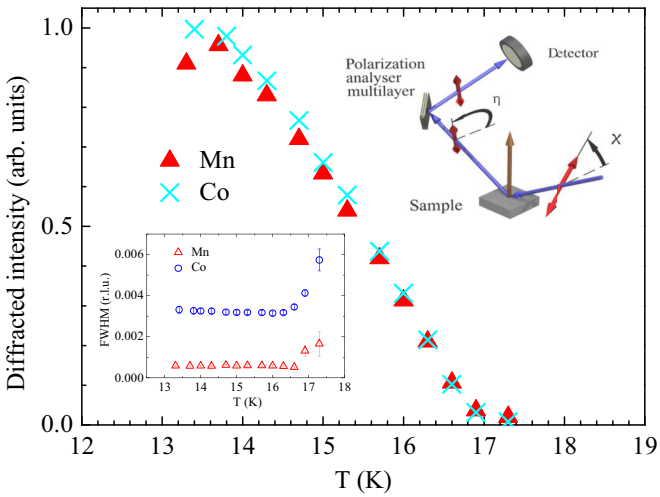

FIG. 2. (Color online) Temperature dependence of the integrated intensity of AF4 (1/2 0 0) magnetic reflection at the maximum of Mn L_2 (655 eV, red solid triangles) for $\chi = 60°$, $\eta = 25°$, and that of Co L_3 (782 eV, blue crosses) in the σ-π' channel, i.e., $\chi = 0°$, $\eta = 90°$. Left inset shows the corresponding FWHM of θ-2θ scans (Mn: red open triangles, Co: blue open circles). Right inset schematically shows the experimental RXMS configuration.

edges arise at $T_N = 17.5$ K, the onset of the AF4 phase on cooling down from the PM region. Their relative intensities evolve similarly and comparably to previous neutron diffraction investigations [15], but the correlation length of the magnetic order for each ion sublattice, as calculated from the full width at half maximum (FWHM) in θ-2θ scans is markedly different, as expected due to the diluted character of the Co content. So, values reach 260(5) nm and 47(1) nm for Mn and Co sublattices, respectively. This corresponds to a ratio of 5.5(2):1, nearly identical to the nominal 85:15 stoichiometric ratio (which yields 5.67:1) of Mn to Co ions in the compound. Near T_N the FWHM values denote a transient zone (16–17.5 K) for both magnetic species, where the long-range order of Mn atoms is more rapidly achieved.

Once the long-range order nature of both magnetic sublattices is demonstrated, the main question arising is regarding the relative orientation of Mn and Co spins. To obtain the answer it is necessary to study in detail the magnetooptical response of the $Mn_{0.85}Co_{0.15}WO_4$ crystal. Thus, we performed a full polarization analysis of the (1/2 0 0) reflection. Briefly, this method relies on the study of the systematic variations of x-ray scattered intensities for a given resonant reflection (either magnetic or originated in the local anisotropy of the electron density distribution) in a material as a function of the relative orientation of the incident and scattered light polarization. X-ray magnetic scattering theory [25,26] points out the tensorial character of the atomic scattering factors, which gets clearly revealed near absorption edges [27,28]. For the F structure factor of AF4 phase (1/2 0 0) reflection near Mn or Co $L_{2,3}$ edges (i.e., for electric dipole transitions) we find $F_{(1/2\,0\,0)} \propto N + (\boldsymbol{\varepsilon}' \times \boldsymbol{\varepsilon})(\mathbf{z}_1\text{-}\mathbf{z}_2)$ (1), with N a scalar accounting for the nonresonant magnetic contribution, and $\boldsymbol{\varepsilon}$, $\boldsymbol{\varepsilon}'$, and $\mathbf{z}_i$ the unit vectors describing the polarization of the incident and scattered light, and the magnetic moment at the i atom site, respectively. The charge scattering amplitude for this propagation vector is strictly zero. Given the collinearity of the antiferromagnetically ordered moments in the AF4 phase, and after having experimentally verified the negligible contribution of the nonresonant magnetic scattering part near the investigated absorption edges, the structure factor gets reduced to $F_{(1/2\,0\,0)} \propto 2\,\mathbf{z}_1\,(\boldsymbol{\varepsilon}' \times \boldsymbol{\varepsilon})$ (2). Thus, the dependence of the scattered intensities (proportional to F^2) on the incident and scattered light electromagnetic vectors, and the (either Mn or Co) element specific moments can get easily modeled.

The experimental (1/2 0 0) scattered intensities at the maximum of the Co L_3 and Mn L_2 edges are plotted in Fig. 3 as a function of the incident and scattered photon beam electric polarization vector in the scattering reference frame [26], respectively denoted by χ and η. The latter is also used to define the orientation of the multilayered analyzer (MA). The experimental dependence follows in both cases a sinusoidal behavior. $\chi = 0^\circ$ and $\chi = 90^\circ$ correspond to an incident beam with σ and p polarization, respectively. Meanwhile, η values of 0° and 90° implies detection of the σ and π channels respectively (provided the orientation of the MA is correspondingly oriented). Thus, $\chi = \eta = 0^\circ$ corresponds to the so-called σ-σ' scattering channel that leads to systematic extinction according to RXMS theory. For this particular case the Co L_3 experimental scattered intensity is zero, as expected for a magnetic reflection (Fig. 3, top).

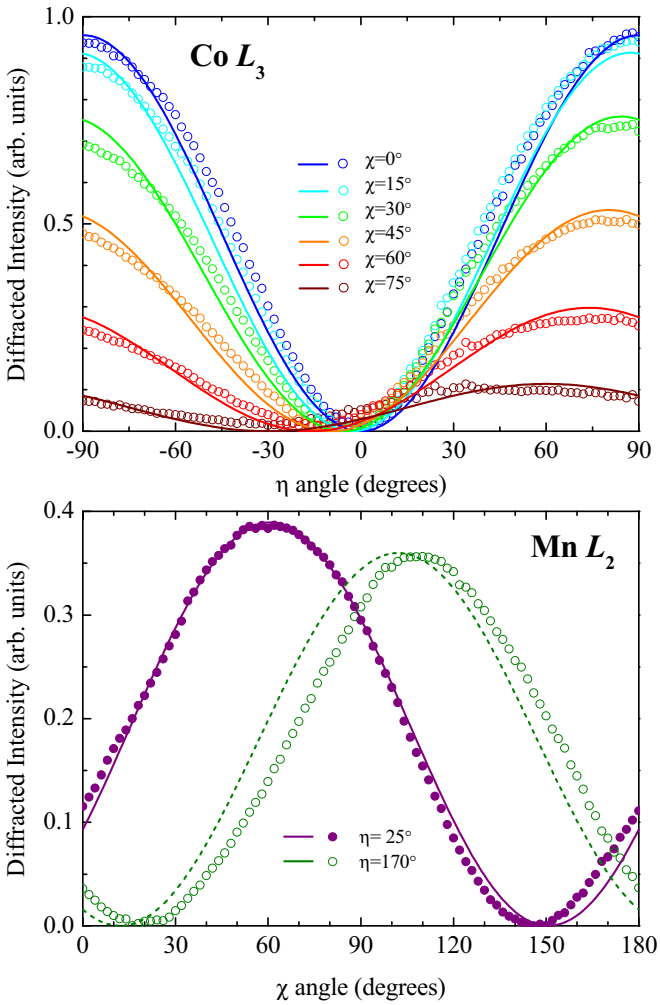

FIG. 3. (Color online) Full polarization analysis of (1/2 0 0) at 13 K. In top panel, the diffracted intensity at the maximum of Co L_3 edge is recorded as a function of η for different values of χ. Alternatively, in bottom panel, the Mn L_2 edge resonant intensity is plotted as a function of χ for two different η positions of the MA.

A zero minimum of the RXMS signal persists for every incident polarization χ moving from 0°–75° but this is found at different, monotonously shifting η positions from 0º to $\approx -30^\circ$, respectively. The polarization analysis at the Mn L_2 edge (Fig. 3, bottom) is less comprehensive due to the previously explained constraints and consists of the (1/2 0 0) intensity variation as a function of the incident light polarization χ for two different orientations η of the analyzer. We fitted the experimental full polarization analysis curves for the AF4 (1/2 0 0) reflection at the Co L_3 and Mn L_2 edges using Eq. (2) for the structure factor, with the orientation of magnetic moments $\mathbf{z}_1$ as the only fitting parameter. Best calculated curves are also shown in Fig. 3. The unitary $\mathbf{z}_1$ vectors are described in standard spherical coordinates by means of θ and φ angles within the crystal reference system, with origin at [0 0 1] and [1 0 0] directions, respectively. For Co, the best fit for the orientation of $\mathbf{z}_1$ yielded $\theta_{Co} = -46(1)^\circ$ [or $+134(1)^\circ$] and $\varphi_{Co} = 3.5(3)^\circ$, respectively. Meanwhile, $\theta_{Mn} = -34(3)^\circ$ [or $+146(3)^\circ$] and $\varphi_{Mn} = 3.7(5)^\circ$ were found for Mn moments. Values in parenthesis are estimated errors in the last digit.

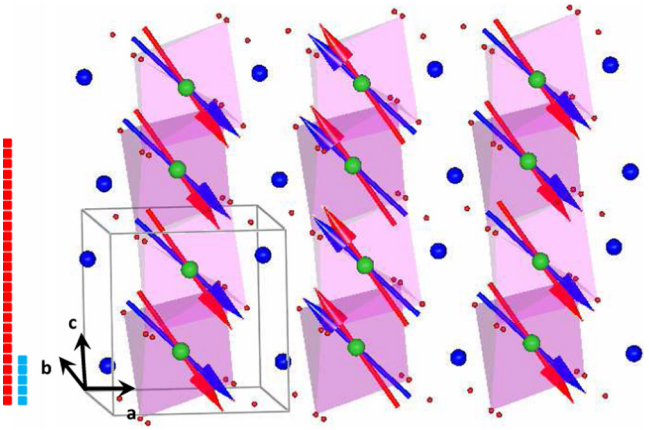

FIG. 4. (Color online) Magnetic order of cobalt (blue) and manganese (red) moments in the AF4 phase of $Mn_{0.85}Co_{0.15}WO_4$, reflecting a noncollinear configuration of the two magnetic species occupying the $2f$ crystallographic site. Green, blue, and red balls stand for Mn/Co, W, and O atoms in the crystal structure. The vertical array of blue and red solid squares represents the relative correlation length of the AF4 order for Mn and Co moments, respectively.

The average magnetic orientation found after considering the relative abundance of Mn and Co in the $2f$ site ($\theta = 144^\circ$ in the ac plane) is, within errors, the same as the average description reported for this phase using neutron diffraction in Refs. [14] ($\theta = 143^\circ$ for $x = 0.20$) and [15] ($\theta = 142^\circ$ for $x = 0.135$ and 0.17). A small misalignment when placing the single crystal on the diffractometer may explain the nonzero φ values reported. Our results are thus consistent with the average moment orientation, expected in the ac plane, and demonstrate that Mn and Co moments form AF sublattices in the AF4 phase. These are not collinear to each other but form an angle of about 12º, as shown in Fig. 4. Noteworthy, the orientation of Co moments we derive is identical to the Co anisotropy axis direction determined by Hollmann *et al.* [18] in $CoWO_4$, and coincides with the direction of Co moments at $T < T_N = 55$ K as reported from single-crystal neutron diffraction [17].

The partial decoupling of Mn and Co moments observed in $Mn_{0.85}Co_{0.15}WO_4$ above T_C is expected to be also present in FE phases of this and other (Mn, Co)WO_4 compounds, assisted by the magnetic anisotropy term in the free energy. Although in most works the behavior of the electric polarization in single-phase MFs is addressed by only considering the average magnetic structure, it is important to recall that the coupling between magnetic moments and polar distortions is of local nature. So it is the antisymmetric Dzyaloshinskii-Moriya (DM) interaction governing polar distortions in most of the new spin-induced MF materials [3]. Therefore, attention must be paid to possible intrinsic deviations at the local scale from the average description. Inhomogeneous FE/magnetic responses to the electric or magnetic fields have to be considered at the local scale also in so-called bulk single-phase MFs with intrinsic inhomogeneities such as the present solid solution.

In summary, using resonant soft x-ray magnetic scattering we have studied the so-called collinear AF4 phase of $Mn_{0.85}Co_{0.15}WO_4$ multiferroic wolframite. This phase thermally precedes the appearance of ferroelectricity and rivals with AF2 cycloidal order in $Mn_{1-x}Co_xWO_4$ compounds with $x \geqslant 0.15$. We have demonstrated that Co moments get long-range magnetically ordered concomitantly to Mn ones. The magnetic correlation length of Mn moments converges to a maximum value of 260(5) nm (about 5.5 times larger than for Co sublattice). Furthermore, we have found that Mn and Co moments are not collinearly oriented to each other but form a relative angle of 12 degrees in $Mn_{0.85}Co_{0.15}WO_4$. The orientation of Co moments corresponds to that previously found in $CoWO_4$ and it is determined by a strong single-ion magnetic anisotropy axis. The magnetocrystalline energy associated to the sites occupied by Co triggers Mn moments (through Co-Mn exchange coupling) to align parallel to the magnetic easy axis of Co ions. But this does not get fully achieved for the composition investigated.

The great sensitivity of the polarization tensor to Co content and the abundance of distinct ferroelectric phases in these isostructural compounds were attributed to the anisotropic features of Co ions and Mn-Co spins exchange interaction. Here we have shown that, due to the strong uniaxial anisotropy of Co^{2+}, the two species of magnetic moments do not behave likewise. The striking element-resolved results presented thus open the door to a deeper reexamination beyond the average magnetic descriptions proposed in the phase diagram of these wolframites, especially at doping levels below $x \sim 0.20$. Among the novel physical phenomena for which a partial magnetic decoupling of Co and Mn sublattices could be relevant, one can mention the control of ferroelectric domains by magnetic fields, tuning the maximum polarization by chemical doping, the control of magnetism at the nanoscale by electric fields, or phase separation phenomena in selected regions of the phase diagram. We cannot exclude the occurrence of a similar noncollinearity of ordered spins from different magnetic ions in other mixed compounds with competing anisotropic interactions.

We are thankful for financial support from MINECO (Spanish government) and the European Community (FEDER) under Projects No. MAT2009-09308, No. MAT2012-38213-C02-02, and No. CSD2007-00041 (NANOSELECT), the Russian Foundation for Basic Research under Project No. 13-02-01093, and the Diamond Light Source for granting beam time. We also thank G. Subías and J. García-Ruiz for valuable discussions.

[1] T. Kimura, T. Goto, H. Shintani, K. Ishizaka, T. Arima, and Y. Tokura, Nature (London) **426**, 55 (2003).

[2] S. W. Cheong and M. Mostovoy, Nat. Mater. **6**, 13 (2007).

[3] H. Katsura, N. Nagaosa, and A.V. Balatsky, Phys. Rev. Lett. **95**, 057205 (2005).

[4] M. Kenzelmann, A. B. Harris, S. Jonas, C. Broholm, J. Schefer, S. B. Kim, C. L. Zhang, S.-W. Cheong, O. P. Vajk, and J. W. Lynn, Phys. Rev. Lett. **95**, 087206 (2005).

[5] K. Taniguchi, N. Abe, T. Takenobu, Y. Iwasa, and T. Arima, Phys. Rev. Lett. **97**, 097203 (2006); **102**, 147201 (2009).

[6] K. Taniguchi, N. Abe, H. Sagayama, S. Otani, T. Takenobu, Y. Iwasa, and T. Arima, Phys. Rev. B **77**, 064408 (2008).

[7] I. Urcelay-Olabarria, E. Ressouche, A. A. Mukhin, V. Yu. Ivanov, A. M. Balbashov, G. P. Vorobev, Yu. F. Popov, A. M. Kadomtseva, J. L. García-Muñoz, and V. Skumryev, Phys. Rev. B **85**, 094436 (2012).

[8] A. H. Arkenbout, T. T. M. Palstra, T. Siegrist, and T. Kimura, Phys. Rev. B **74**, 184431 (2006).

[9] I. Urcelay-Olabarria, E. Ressouche, A. A. Mukhin, V. Yu. Ivanov, A. M. Kadomtseva, Yu. F. Popov, G. P. Vorob'ev, A. M. Balbashov, J. L. García-Muñoz, and V. Skumryev, Phys. Rev. B **90**, 024408 (2014).

[10] G. Lautenschlager, H. Weitzel, T. Vogt, R. Hock, A. Bohm, M. Bonnet, and H. Fuess, Phys. Rev. B **48**, 6087 (1993).

[11] I. Urcelay-Olabarria, J. L. García-Muñoz, E. Ressouche, V. Skumryev, V. Yu. Ivanov, A. A. Mukhin, and A. M. Balbashov, Phys. Rev. B **86**, 184412 (2012).

[12] F. Ye, Y. Ren, J. A. Fernandez-Baca, H. A. Mook, J. W. Lynn, R. P. Chaudhury, Y. Q. Wang, B. Lorenz, and C. W. Chu, Phys. Rev. B **78**, 193101 (2008).

[13] Y.-S. Song, J.-H. Chung, J. M. S. Park, and Y.-N. Choi, Phys. Rev. B **79**, 224415 (2009).

[14] I. Urcelay-Olabarria, E. Ressouche, A. A. Mukhin, V. Yu. Ivanov, A. M. Balbashov, J. L. García-Muñoz, and V. Skumryev, Phys. Rev. B **85**, 224419 (2012).

[15] F. Ye, S. Chi, J. A. Fernandez-Baca, H. Cao, K.-C. Liang, Y. Q. Wang, B. Lorenz, and C. W. Chu, Phys. Rev. B **86**, 094429 (2012); K.-C. Liang, Y.-Q. Wang, Y. Y. Sun, B. Lorenz, F. Ye, J. A. Fernandez-Baca, H. A. Mook, and C. W. Chu, New J. Phys. **14**, 073028 (2012).

[16] I. Urcelay-Olabarria, J. M. Perez-Mato, J. L. Ribeiro, J. L. Garcia-Muñoz, E. Ressouche, V. Skumryev, and A. A. Mukhin, Phys. Rev. B **87**, 014419 (2013).

[17] J. B. Forsyth and C. Wilkinson, J. Phys.: Condens. Matter **6**, 3073 (1994).

[18] N. Hollmann, Z. Hu, T. Willers, L. Bohatý, P. Becker, A. Tanaka, H. H. Hsieh, H.-J. Lin, C. T. Chen, and L. H. Tjeng, Phys. Rev. B **82**, 184429 (2010).

[19] Collinear AF1 order reappears in a narrow range around $T = 10\,\mathrm{K}$, $x = 0.12$, where exchange and magnetocrystalline anisotropy terms induce maximum frustration.

[20] R. P. Chaudhury, F. Ye, J. A. Fernandez-Baca, Y.-Q. Wang, Y. Y. Sun, B. Lorenz, H. A. Mook, and C. W. Chu, Phys. Rev. B **82**, 184422 (2010).

[21] T. A. W. Beale, T. P. A. Hase, T. Iida, K. Endo, P. Steadman, A. R. Marshall, S. S. Dhesi, G. Van der Laan, and P. D. Hatton, Rev. Sci. Instrum. **81**, 073904 (2010).

[22] C. Mazzoli, S. B. Wilkins, S. Di Matteo, B. Detlefs, C. Detlefs, V. Scagnoli, L. Paolasini, and P. Ghigna, Phys. Rev. B **76**, 195118 (2007).

[23] J. Okamoto, K. Horigane, H. Nakao, K. Amemiya, M. Kubota, Y. Murakami, and K. Yamada, J. Phys: Conf. Ser. **425**, 202003 (2013).

[24] J. Okamoto, H. Nakao, Y. Yamasaki, H. Wadati, A. Tanaka, M. Kubota, K. Horigane, Y. Murakami, and K. Yamada, J. Phys. Soc. Jpn. **83**, 044705 (2014).

[25] J. P. Hannon, G. T. Trammell, M. Blume, and D. Gibbs, Phys. Rev. Lett. **61**, 1245 (1988).

[26] J. P. Hill and D. F. McMorrow, Acta Crystallogr. Sect. A **52**, 236 (1996).

[27] D. H. Templeton and L. K. Templeton, Phys. Rev. B **49**, 14850 (1994).

[28] V. E. Dmitrienko, K. Ishida, A. Kirfel, and E. N. Ovchinnikova, Acta Crystallogr. Sect. A **61**, 481 (2005).